X-ray and SEM studies on zirconia powders

G. Dercz *, K. Prusik, L. Pająk

Institute of Materials Science, University of Silesia,
ul. Bankowa 12, 40-007 Katowice, Poland
* Corresponding author: E-mail address: gdercz@op.pl

Methodology of research

ABSTRACT

Purpose: The microstructure characterization of commercially available zirconia powders was the purpose of this paper. Different methods of structure analysis were applied owing to the complex, multiphase structure of studied materials.

Design/methodology/approach: The X-ray diffraction (XRD) and scanning electron microscopy (SEM) investigations were performed on three commercial zirconia ceramic materials: Amdry 204 NS (ZrO_2^- 8 wt.% of Y_2O_3), Metco C8 YZ (ZrO_2^- 8 wt.% of Y_2O_3) and Metco 202 (ZrO_2^- 20 wt.% of Y_2O_3). The Rietveld method appeared to be very useful in the verification of the qualitative phase composition and in the determination of phase abundance. Hill and Howard procedure was applied for quantitative phase analysis. The parameters of the individual diffraction line profiles were determined by PRO-FIT Toraya procedure. The powder morphology was analyzed by SEM method.

Findings: In the Amdry sample comparable contents of two phases: monoclinic (44.1 wt.%) and cubic (55.9 wt.%) was stated by XRD analysis. The presence of Y2O3 phase besides of monoclinic, tetragonal and cubic ZrO_2 ones were stated for both Metco samples. The tetragonal phase (55.2 wt.%) was found to be the main component of the Metco C8-YZ sample whereas the content of Y_2O_3 is the lowest (2.7 wt.%). On the other hand cubic phase (68.2 wt.%) was the main component of the Metco 202 sample and the content of Y_2O_3 is again the lowest (4.5 wt.%). The SEM images of all the samples reveal the spherical shape of powder particles. The morphology of both Metco samples is quite similar. For Metco 202 sample the hierarchical type structure of powder particle is observed; the greater particles contain smaller ones. The shell of particles is composed of distinct patches. On the other hand the structure of spherical particles of Amdry sample is of branched, rather dense skeleton type. From X-ray diffraction data it can be concluded that the crystallite size of all involved phases lies above nanoscale.

Practical implications: Performed studies enable the determination of the relation between the microstructure of commercial powders and their utilisable properties.

Originality/value: The applied, different methods of structure analysis appeared to be very useful in the microstructure analysis of complex, multiphase material.

Keywords: X-ray Phase Analysis; Electron Microscopy; Rietveld method; Toraya procedure; Ceramics

1. Introduction

Ceramic materials based on zirconia owing to their properties are of widespread application [9]. Three polymorphic forms of pure zirconia were found in equilibrium state: monoclinic – below ~1170°C, tetragonal – in the temperature range ~1170–2370°C and cubic – above ~2370°C. Zirconia forms of higher symmetry have properties very often preferable to ones of monoclinic form. Usually yttrium oxide is used as the stabilization component of higher symmetry zirconia forms [25]. Nanotechnology of ceramic materials based on zirconia is now of great interesting [1,4,10,22].
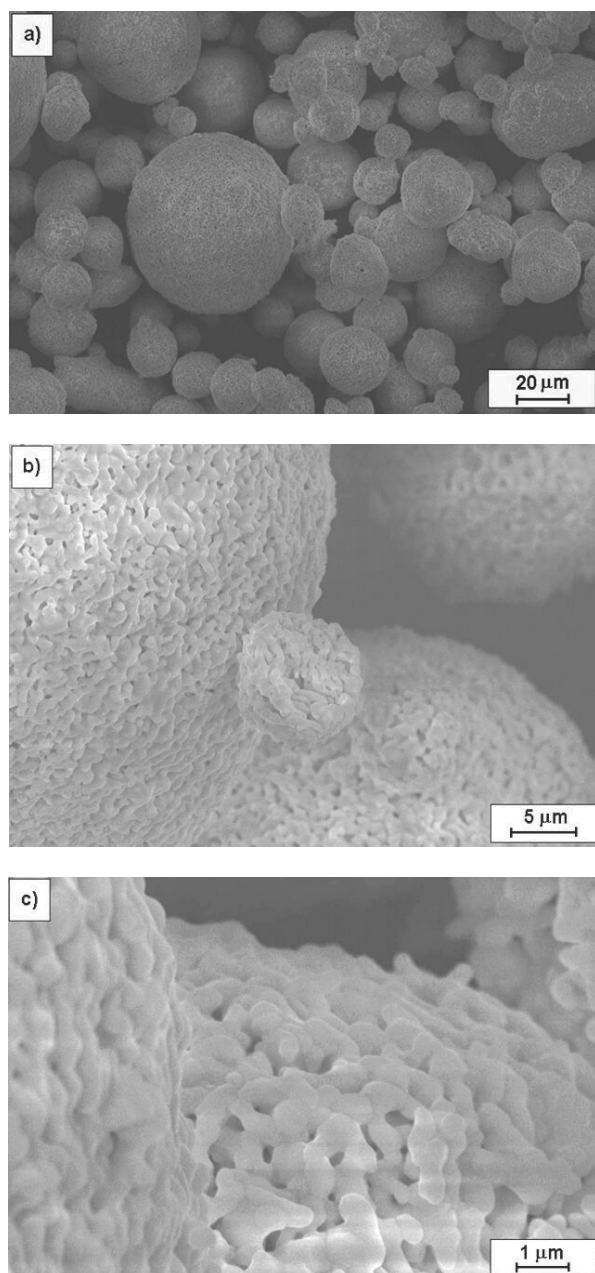
Fig. 1. SEM images of Amdry-8 sample

At present the X-ray diffraction and electron microscopy methods are standard ones in the microstructure characterization of complex, multiphase materials. X-ray diffraction methods enable qualitative and quantitative phase analysis and also microstructure characterization (crystallite sizes, lattice distortions, dislocation densities, stacking faults and twins probability [16]).

The purpose of the present work is the microstructure characterization of three commercially available, zirconia-based materials using XRD (X-Ray Diffraction) and SEM (Scanning Electron Microscopy) methods.

The analysis of XRD patterns was performed by the use of Rietveld method [15,23,24] and Toraya procedure [19-21]. The detailed information on the structure of concerned phases is necessary for the estimation of phase abundance in multiphase materials [16]. The procedure of quantitative phase analysis based on the values of scale factors determined by Rietveld refinement was introduced by Hill and Howard [8]. Rietveld method appeared to be useful in the microstructure characterization and also in the verification of the qualitative phase composition of multiphase materials [2,3,5-7,11-14,17,18].

The powder morphology of studied materials was analyzed by SEM method.

2. Material and research methodology

The structure investigations were performed on three commercial zirconia materials: Amdry 204 NS ($ZrO_2 - 8$ wt.% of Y_2O_3), Metco C8-YZ ($ZrO_2 - 8$ wt.% of Y_2O_3) and Metco 202 ($ZrO_2 - 20$ wt.% of Y_2O_3), hereafter called Amdry-8, Metco-8 and Metco-20, respectively.

The collection of X-ray diffraction patterns was performed by the use X-Pert Philips diffractometer equipped with curved graphite monochromator on diffracted beam and with the following slits (in the sequence from Cu tube to counter); Soller (2°), divergence ($1/2^o$), antiscatter ($1/2^o$), Soller (2°) and receiving (0.15 mm). The X-ray data collection was performed in $20-150^o$ 2θ range with 0.04^o step. The time of data acquisition was chosen to obtain the intensity of the most intense diffraction line of ~20 000 counts for all X-ray patterns.

Toraya PRO-FIT procedure, which applies Pearson VII function for the description of line profiles was used for the determination of the profile parameters of the individual diffraction lines.

The Rietveld analysis was performed applying DBWS-9807 program that is an update version of the DBWS programs for Rietveld refinement with PC and mainframe computers.

The calculated intensities y_{ci} are determined by summing the contributions from neighbouring Bragg reflections plus the background:

$$y_{ci} = s \sum_k L_k |F_k|^2 \phi(2\theta_i - 2\theta_k) P_k A + y_{bi}$$

(1)

where:
S – the scale factor,
k – represents the Miller indices, h, k, l for the Bragg reflection,
L_k – the Lorentz, polarization and multiplicity factors,
ϕ - the reflection profile function,
P_k – the preferred orientation,
A – the absorption factor,
F_k - the structure factor for the k-th Bragg reflection,
y_{bi} - the background intensity at the i-th step.

The pseudo-Voigt function was applied for the describing of diffraction line profiles during Rietveld refinement. The quality of the fit of calculated to experimental diffraction data was monitored by R_{wp} (weighted-pattern factor) and S (goodness-of-fit) parameters [16].

$$R_{wp} = \left[\frac{\sum_i w_i (y_i - y_{ci})^2}{\sum_i w_i (y_i)^2} \right]^{1/2} \cdot 100\%$$

(2)

$$R_{exp} = \left[\frac{N - P}{\sum_i w_i y_i} \right]^{\frac{1}{2}} \cdot 100\%$$

(3)

$$S = \frac{\sum_i w_i (y_i - y_{ci})^2}{N - P}$$

(4)

where:

y_i – the experimental intensities,

y_{ci} – the calculated intensities,

$w_i = (1/y_i)$ – the weight experimental observations,

N – the number of experimental observations,

P – the number of fitting parameters.

The process of successive profile refinements modulates different structural and microstructural parameters of the simulated pattern to fit the experimental diffraction pattern. Profile refinement continues until convergence is reached in each case, with the value of the quality factor (S) approaching 1.

The phase abundance was determined using the relation proposed by Hill and Howard[24]:

$$W_p = \frac{S_p (Z \cdot M \cdot V)}{\sum_{i=1}^{n} S_i (Z \cdot M \cdot V)_i} \cdot 100\%$$

(5)

where:

W_p – relative weight fraction of phase p in the mixture of n phases (wt. %),

S – Rietveld scale factor,

Z – number of formula units per unit cell,

M – mass of the formula unit (in atomic mass units),

V – unit cell volume (in Å^3).Morphology of the powder particles was analyzed using SEM (JEOL JSM-6480) method.

3. Results and discussion

Scanning electron microscopy images reveal the spherical shape of powder particles for all studied samples (Figs. 1-3). Differences in their morphology can be found from the analysis of the corresponding images obtained at different magnification. For Amdry-8 sample the particle size distributions looks like bimodal with preferable particle sizes of ~20 µm and ~40 µm. The image presented in Fig. 1c indicates the branched, rather dense, skeleton type structure of Amdry-8 powder particles with backbone thickness of ~0.5 µm.

The SEM images of the Metco samples (Figs. 2 and 3) show generally the similar morphology of their powder particles. The surface layer of particles is slightly folded and is covered by distinct patches (Figs. 2c and 3c). The particle size distributions of both Metco powders is rather broad with particle diameters in the range from ~8 µm to ~70 µm. For Metco-20 powder (Fig. 3a) the hierarchical structure type of greater particles can be postulated; the greater particles contain the smaller ones. Such type of structure cannot be excluded for Metco-8 sample but is less probable for Amdry-8 one.
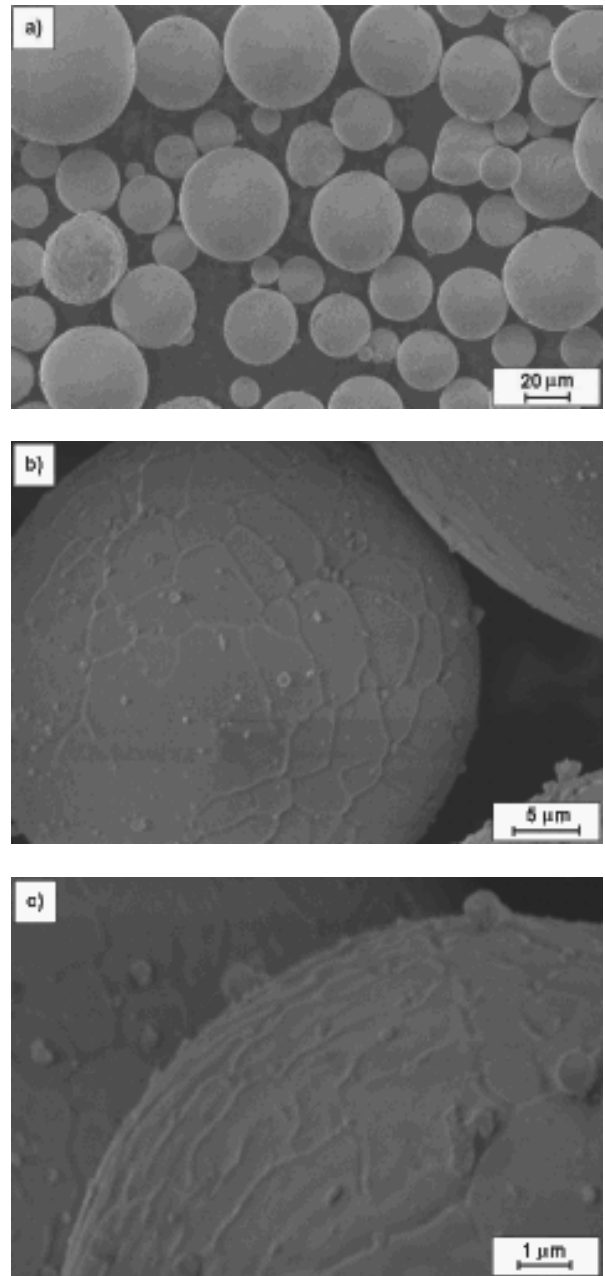

Fig. 2. SEM images of Metco-8 sample

Analysis of the X-ray diffraction pattern of Amdry-8 sample reveals the presence of monoclinic and cubic zirconia phases (Fig. 4). In both Metco samples the monoclinic, tetragonal and cubic ZrO_2 phases and Y_2O_3 one were found (Figs. 5 and 6).

The contents of all involved phases determined by Hill and Howard procedure [24] are presented in Tables 1-3. The accuracy of the determination of phase contents is difficult to estimation but should be relatively high because the main components of the studied materials are the phases of the same absorption

coefficient. Comparatively loose structure of powder particles and particle sizes enable their good penetration by X-rays. In Amdry-8 sample the contents of both cubic and monoclinic zirconia phases are comparable and equal to ~55.9 and ~44.1 wt.%, respectively; the presence of Y_2O_3 phase was not found by X-ray diffraction.
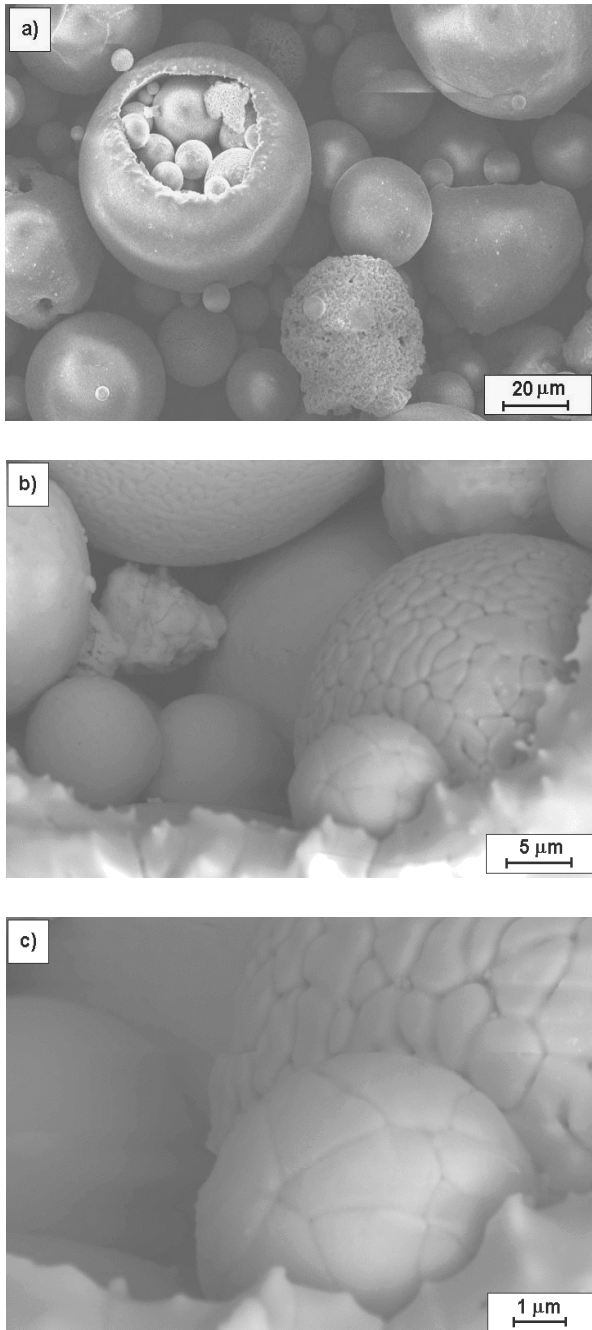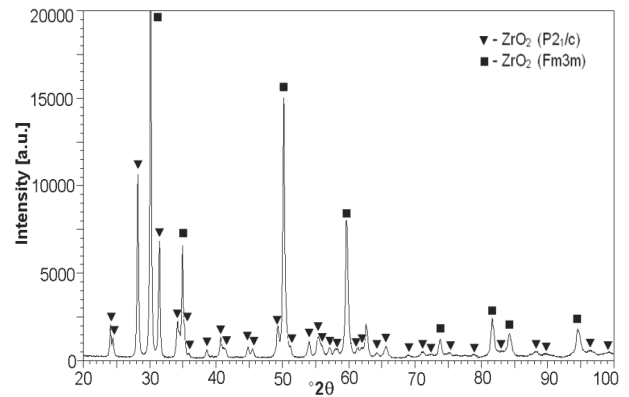

Fig. 3. SEM images of Metco-20 sample

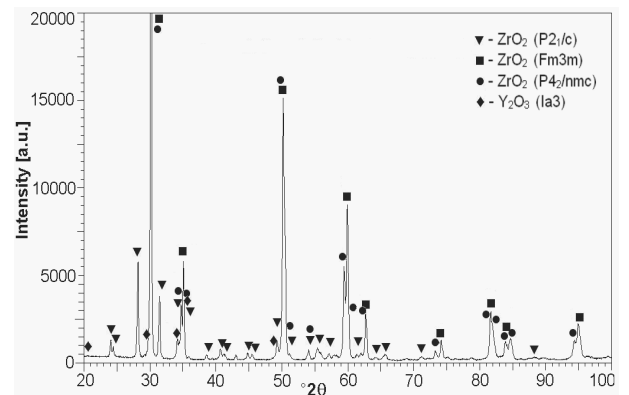Fig. 4. X-ray diffraction pattern of Amdry-8 sample

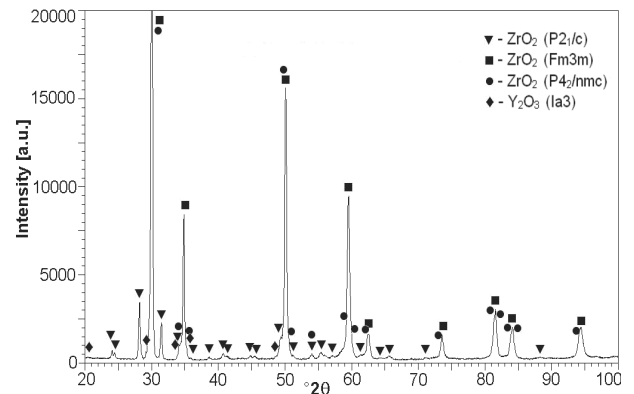Fig. 5. X-ray diffraction pattern of Metco-8 sample

Fig. 6. X-ray diffraction pattern of Metco-20 sample

The tetragonal zirconia phase appeared to be the main component of Metco-8 sample (55.2 wt.%). The content of cubic form is still relative high (36.6 wt.%) whereas of tetragonal one is relatively low (7.5 wt.%); the content of Y_2O_3 phase is the lowest (2.7 wt.%). Thus, above results indicate high contents of high symmetrical zirconia phases in Metco-8 sample.

The cubic zirconia phase appeared to be the main component of Metco-20 sample (68.2 wt.%). The content of monoclinic zirconia phase is relative high and equal to 22.3 wt.%. The contents of tetragonal zirconia phase and Y_2O_3 one are comparable and relatively low (5.0 and 4.5 wt.% respectively).

Table 1.
Lattice parameters and the contents of components for Amdry-8 sample (8 wt.% of Y_2O_3)

Phase	Space group	Lattice parameters [nm]		Contents [wt.%]
		Rietveld	ICDD	
ZrO$_2$	P2$_1$/c	$a_0 = 0.51571(8)$	$a_0 = 0.51507(4)$	44.1
		$b_0 = 0.52046(8)$	$b_0 = 0.52028(4)$	
		$c_0 = 0.53154(8)$	$c_0 = 0.53156(4)$	
		$\beta = 99.191°$	$\beta = 99.196°$	
ZrO$_2$	Fm3m	$a_0 = 0.51364(8)$	$a_0 = 0.5128$	55.9

Table 2.
Lattice parameters and the contents of components for Metco 1 sample (8 wt.% of Y_2O_3)

Phase	Space group	Lattice parameters [nm]		Contents [wt.%]
		Rietveld	ICDD	
ZrO$_2$	P2$_1$/c	$a_0 = 0.51583(8)$	$a_0 = 0.51507(4)$	7.5
		$b_0 = 0.52058(8)$	$b_0 = 0.52028(4)$	
		$c_0 = 0.53186(8)$	$c_0 = 0.53156(4)$	
		$\beta = 99.23°$	$\beta = 99.196°$	
ZrO$_2$	Fm3m	$a_0 = 0.51350(8)$	$a_0 = 0.5128$	36.6
ZrO$_2$	P4$_2$/nmc	$a_0 = 0.36136(6)$	$a_0 = 0.35961(1)$	55.2
		$c_0 = 0.51653(8)$	$c_0 = 0.51843(2)$	
Y$_2$O$_3$	Ia3	$a_0 = 1.0610(2)$	$a_0 = 1.0604(5)$	2.7

Table 3.
Lattice parameters and the contents of components for Metco 2 sample (20 wt.% of Y_2O_3)

Phase	Space group	Lattice parameters [nm]		Contents [wt.%]
		Rietveld	ICDD	
ZrO$_2$	P2$_1$/c	$a_0 = 0.51582(8)$	$a_0 = 0.51507(4)$	22.3
		$b_0 = 0.52064(8)$	$b_0 = 0.52028(4)$	
		$c_0 = 0.53184(8)$	$c_0 = 0.53156(4)$	
		$\beta = 99.25°$	$\beta = 99.196°$	
ZrO$_2$	Fm3m	$a_0 = 0.51490(8)$	$a_0 = 0.5128$	68.2
ZrO$_2$	P4$_2$/nmc	$a_0 = 0.36667(6)$	$a_0 = 0.35961(1)$	5.0
		$c_0 = 0.52381(8)$	$c_0 = 0.51843(2)$	
Y$_2$O$_3$	Ia3	$a_0 = 1.0605(2)$	$a_0 = 1.0604(5)$	4.5

The low content of Y_2O_3 phase (4.5 wt.%) means that meaning part of this phase is intercorporated into zirconia phases (nominal content of Y_2O_3 phase in Metco-20 sample is 20 wt.%).

The crystallite size of all phases found in studied materials lies above nanoscale.

The values of lattice parameters determined by Rietveld method and these found in ICDD files for all concerned phases are given in Tables 1-3; generally good agreement between them can be seen. The accuracy of the lattice parameter determination (equal to ±0.015%) was estimated using SRM 1976 alumina plate as a standard.
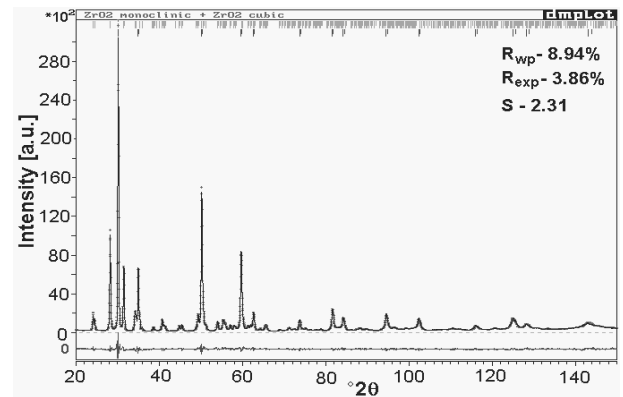

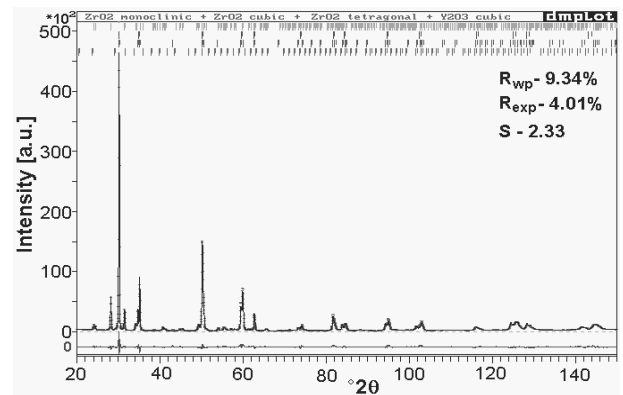Fig. 7. Rietveld output of X-ray diffraction pattern for Amdry-8 sample

Fig. 8. Rietveld output of X-ray diffraction pattern for Metco-8 sample
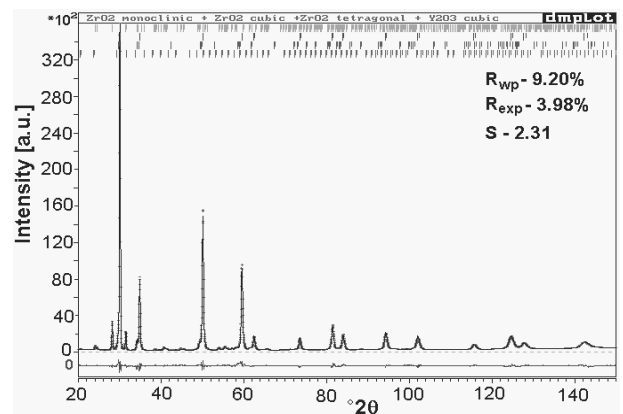

Fig. 9. Rietveld output of X-ray diffraction pattern for Metco-20 sample

The values of lattice parameters of all zirconia phases are very close (Tables 1-3); moreover the lattice constant of Y_2O_3 phase are about twice of these of zirconia phases. It means the overlapping of diffraction lines of all phase present in studied

materials. The Rietveld method by the analysis of the whole diffraction patterns enables good separation of diffraction lines and thus appears especially useful in the analysis of actually studied materials. The Rietveld refinement plots for studied samples are presented in Figs. 7-9. The goodness of fitting of calculated patterns to the experimental ones can be regarded as satisfactory.

4. Conclusions

- Scanning electron images reveal the spherical shape of powder particles for all studied samples. The structure of powder particles of Amdry-8 sample is of branched, dense, skeleton type. The morphology of both Metco samples is quite similar but different to observed for Amdry-8 sample. The surface of powder particles is slightly folded and is covered by distinct patches. The hierarchical structure type of greater particles is observed for Metco-20 sample; the greater particles contain the smaller ones.
- In Amdry-8 sample the cubic and monoclinic zirconia phases are present and their contents are comparable and equal to 55.9 and 44.1 wt.%, respectively. The presence of four phases: cubic, tetragonal and monoclinic zirconia and Y_2O_3, in both Metco samples, was stated. It was found that in Metco-8 sample the content of tetragonal zirconia phase is the highest (55.2 wt.%), whereas of Y_2O_3 one is the lowest (2.7 wt.%). The content of monoclinic zirconia is relatively low (7.5 wt.%). In Metco-20 sample the content of cubic zirconia phase is the highest (68.2 wt.%), whereas of Y_2O_3 one is the lowest (4.5 wt.%). The content of monoclinic zirconia phase is still relative high (22.3 wt.%).
- The crystallite size of all phases found in studied materials lies above nanoscale. Good agreement of lattice parameters determined by Rietveld refinement method and these from ICDD files was obtained for all involved phases.
- Rietveld refinement method and PRO-FIT Toraya procedure appeared to be very useful in the characterization of complex, multiphases materials.

Acknowledgements

References

[1] U. Betz, A. Sturm, J.F. Loeffler, W. Wagner, A. Wiedenmann, H. Hahn, Low-temperature isothermal sintering and microstructural characterization of nanocrystalline zirconia ceramics using small angle neutron scattering, Nanostructured Materials 12 (1999) 689-692.

[2] D.L. Bish, S.A. Howard, Quantitative phase analysis using the Rietveld method, Journal of Applied Crystallography 21 (1988) 86-91.

[3] D.L. Bish, J.E. Post, Quantitative mineralogical analysis using the Rietveld full-pattern fitting method, American Mineralogist 78 (1993) 932-940.

[4] X. Bokhimi, A. Morales, O. Novaro, M. Portilla, T. Lopez, F. Tzoompantzi, R. Gomez, Tetragonal nanophase stabilization in nondoped Sol–Gel zirconia prepared with different hydrolysis catalysts, Journal of Solid State Chemistry 135 (1998) 28-35.

[5] G. Dercz, B. Formanek, K. Prusik, L. Pająk, Microstructure of Ni(Cr)-TiC-Cr$_3$C$_2$-Cr$_7$C$_3$ composite powder, Journal of Materials Processing Technology 162-163 (2005) 15-19.

[6] G. Dercz, B. Formanek, K. Prusik, L. Pająk, Microstructure of Ni(Cr)-TiC-Cr$_3$C$_2$-Cr$_7$C$_3$ composite powder, Proceedings of the 13th Scientific International Conference "Achievements in Mechanical and Materials Engineering" AMME'2005, Gliwice−Zakopane, 2005, 99-102.

[7] G. Dercz, K. Prusik, L. Pająk, Structure investigations of commercial zirconia ceramic powder, Journal of Achievements in Materials and Manufacturing Engineering 18 (2006) 259-262.

[8] R.J. Hill, C.J. Howard, Quantitative phase analysis from neutron powder diffraction data using the Rietveld method, Journal of Applied Crystallography 20 (1987) 467-474.

[9] W. Kurzweg, R.B. Heimann, T. Troczyński, M.L. Waymann, Development of plasma – sprayed bioceramic coatings with bond coats based on titania and zirconia, Biomaterials 19 (1998) 1507-1511.

[10] R. Nitsche, M. Winterer, H. Hahn, Structure of nano-crystalline zirconia and yttria, Nanostructured Materials 6 (1995) 679-682.

[11] B.H. O'Connor, M.D. Raven, Applications of the Rietveld refinement procedure in assaying powdered mixtures, Powder Diffraction,3 (1988) 2-6.

[12] L. Pająk, B. Formanek, G. Dercz, Rietveld analysis of intermetallic phases from Ni-Al system, Proceedings of the 11th Scientific International Conference "Achievements in Mechanical and Materials Engineering" AMME'2002, Gliwice−Zakopane, 2002, 405-408.

[13] L. Pająk, B. Formanek, G. Dercz, Dispersion analysis of NiAl-TiC-Al$_2$O$_3$ composite powder, Proceedings of the 12th Scientific International Conference "Achievements in Mechanical and Materials Engineering" AMME'2003, Gliwice−Zakopane, 2003, 723-726.

[14] L. Pająk, B. Formanek, G. Dercz, Dispersion analysis of NiAl-TiC-Al$_2$O$_3$ composite powder ground in high-energy attritorial mill, Journal of Materials Processing Technology 175 (2006) 334-337.

[15] H.M. Rietveld, A profile refinement method for nuclear and magnetic structures, Journal of Applied Crystallography 2 (1969) 65-711.

[16] R.L. Snyder, J. Fiala, H.J. Bunge, Defects and microstructure analysis by diffraction, EDS IUCr Monographs on Crystallography 10, Oxford University Press Inc., New York, 1999.

[17] J.C. Taylor, Computer programs for standardless quantitative analysis of minerals using the full powder diffraction profile, Powder Diffraction 6 (1991) 2-9.

[18] J.C. Taylor, C.E. Matulis, Use of a universally measured standard profile for Rietveld quantification of montmorillonites, Powder Diffractometry 9 (1994) 119-123.

[19] H. Toraya, Array type universal profile function for powder pattern fitting, Journal of Applied Crystallography 19 (1986) 485-491.

[20] H. Toraya, Whole-Powder-Pattern Fitting without reference to a structural model application to X-ray powder diffractometer data, Journal of Applied Crystallography 19 (1986) 440-447.

[21] H. Toraya, Whole-Powder-Pattern decomposition method, The Rigaku Journal 6 (1989) 28-34.

[22] J.A. Wang, M.A. Valenzuela, J. Salmones, A. Vazquez, A. Garcia-Ruiz, X. Bokhimi, Comparative study of nanocrystalline zirconia prepared by precipitation and sol-gel methods, Catalysis Today 68 (2001) 21-30.

[23] R.A. Young, D.B. Wiles, Application of the Rietveld methods for structure refinement with powder diffraction data, Advances in X-Ray Analysis 24 (1980) 1-23.

[24] R.W. Young, The Rietveld method, IUCr Monograph on Crystallography, Oxford Science Publishing, 1993.

[25] W.Z. Zhu, Effect of cubic phase on the kinetics of the isothermal tetragonal to monoclinic transformation in $ZrO_2(3mol\%Y_2O_3)$ ceramics, Ceramics International 24 (1998) 35-43.